Characterization of the Transport of Uracil across Caco-2 and LLC-PK_1 Cell Monolayers

Hong Li,[1] Suk-Jae Chung,[1] and Chang-Koo Shim[1,2]

Received June 10, 2002; accepted July 2, 2002

Purpose. The purpose of this study was to characterize the transport of uracil, a pyrimidine nucleobase, in Caco-2 and LLC-PK_1 cells.
Methods. Caco-2 and LLC-PK_1 cells were grown to confluency on a permeable polycarbonate membrane insert to permit transport and uptake experiments after the loading of uracil on either the apical or basolateral side.
Results. The vectorial transport of uracil in both directions was saturable with comparable K_m and V_{max} in Caco-2 cell monolayers, probably because of a Na^+-independent transport system located on the basolateral membrane. In LLC-PK_1 cell monolayers, two distinct transport systems, namely a Na^+-dependent and a Na^+-independent, were functional in the apical to basolateral (A-B) transport of uracil. The first system was saturable with a K_m value of 3.67 ± 0.40 μM, a V_{max} of 11.31 ± 0.91 pmol/cm^2/min, and a Na^+:uracil coupling stoichiometry of 1.28 ± 0.20. The second system was Na^+ independent and satuable with a low affinity (K_m, 50.37 ± 9.61 μM) and V_{max} (16.01 ± 4.48 pmol/cm^2/min). The two transport systems appeared to be located on the apical membrane.
Conclusion. The mechanism of uracil transport differs depending on cell lines; a Na^+-independent system on the basolateral membrane in Caco-2 cells and both Na^+-dependent and Na^+-independent systems on the apical membrane in LLC-PK_1 cells seem to be responsible for the difference.

KEY WORDS: uracil; pyrimidine nucleobase, transport; Caco-2; LLC-PK_1.

INTRODUCTION

Nucleobase analogs are currently in widespread use as antineoplastic and antiviral agents (1,2), and clinical applications of nucleobases are expanding. With widespread applications of combinatorial chemistry in the development of new drugs, the chances for the full realization of the therapeutic potential of these types of compounds are increasing. For example, a pyrimidine analog, YH1885, is expected to soon be in use as a reversible proton pump inhibitor, on the basis of its reversible binding to the K^+-binding site of the pump (3). The success of combinatorial chemistry in terms of new drug discovery is largely a function of the availability of suitable high-throughput screening systems. In the area of gastrointestinal (GI) absorption screening, an estimation of transport across Caco-2 cell monolayers is one of the most widely accepted high-throughput procedures. In addition to GI absorption, renal salvage is also of interest with regard to the maintenance of physiologic functions of normal cells (in the case of nucleobases) or their availability in target cells (in the case of nucleobase analog drugs). Thus, modulation of the influx or efflux across the intestinal epithelium and/or the renal epithelium would be expected to have a major influence on the pharmacokinetics (GI absorption and/or renal excretion) of these compounds (4–7), leading to modified effectiveness, in terms of their use in chemotherapy of tumors (8) and viral infections (9).

Both facilitated diffusion and a Na^+-dependent system have been demonstrated for the transport of nucleobases in a range of tissues and cell lines (10). However, some controversy exists regarding the contribution of the Na^+-dependent system. For example, a Na^+-dependent nucleobase transport system has been demonstrated to be responsible for the transport of pyrimidine nucleobases in rat jejunal tissue rings (11–13) and everted sacs (14) but does not seem to be involved in the uptake of 5-fluorouacil into the intestinal brush border membrane vesicles (14). A Na^+-dependent nucleobase transport system, which is distinct from that in rabbit choroid plexus (15,16), has also been reported in LLC-PK_1 cells (17,18).

In the present study, we report on an investigation of the transport characteristics of uracil, a representative pyrimidine nucleobase, using a human carcinoma cell line, Caco-2 cells, and a pig renal epithelial cell line, LLC-PK_1 cells. These cell culture systems were selected because they are likely to be used in estimating the intestinal absorption (i.e., Caco-2 cells) and renal function (i.e., LLC-PK_1 cells) of nucleobases.

MATERIALS AND METHODS

Materials

[^{3}H]Uracil (2.2 ci/mmol) and [^{14}C]mannitol (50 mci/mmol) were purchased from New England Nuclear (Boston, MA, USA). Fetal bovine serum was purchased from Hyclone Laboratories (Logan, UT, USA). Trypsin-EDTA was purchased from Gibco Laboratories (Gaithersburg, MD, USA). Dulbecco's Modified Eagle's medium, non-essential amino acid solution, L-glutamine, penicillin-streptomycin, Hank's balanced salt solution (HBSS), and *N*-2-hydroxyethylpiperazine-*N*′-2-ethanesulfonic acid (HEPES) were purchased from Sigma Chemical Co. (St. Louis, MO, USA). All other reagents were of analytical grade.

Cell Culture

Caco-2 cells (passage 36-45, American Type Culture Collection, Rockville, MD, USA) were cultured as described previously (19). LLC-PK_1 cells (passage 220-230, American Type Culture Collection) were cultured in Dulbecco's Modified Eagle's medium containing 10% fetal bovine serum, a 1% non-essential amino acid solution, 4 mM L-glutamine, 100 units/mL penicillin, and 0.1 mg/mL streptomycin at 37°C in an atmosphere of 5% CO_2 and 90% relative humidity. For the transport experiments, cells were grown on a permeable polycarbonate insert (1 cm^2, 0.4-μm pore size: Corning Costar Corp., Cambridge, MA, USA) in 12-Transwell plates, and the medium was changed at a 2-day interval. The transepithelial electrical resistance values reached 300–600 Ω·cm^2 for the Caco-2 cell monolayers at 18–25 days of culture (19) and

[1] Department of Pharmaceutics, College of Pharmacy, Seoul National University, 599 Kwanak-Ro, Kwanak-Gu, Seoul 151-742, Korea.
[2] To whom correspondence should be addressed. (e-mail: shimck@plaza.snu.ac.kr)

0724-8741/02/1000-1495/0 © 2002 Plenum Publishing Corporation

145–170 $\Omega \cdot cm^2$ for the LLC-PK_1 cell monolayers at 5 days of culture.

Measurement of Transepithelial Transport of Uracil

The transepithelial transport of uracil across Caco-2 and LLC-PK_1 cell monolayers was measured in the presence or absence of Na^+. The Na^+-containing incubation medium used in the transport study was HBSS buffer supplemented with 20 mM of glucose, 9 mM of sodium bicarbonate, and 25 mM of HEPES (pH 7.4). The concentration of Na^+ in the Na^+-containing incubation medium was 140 mM. The Na^+-free incubation medium was prepared by replacing NaCl and $NaHCO_3$ with equimolar N-methyl-D-glutamine and $KHCO_3$ in the HBSS buffer. The pH of the medium was adjusted by adding NaOH or KOH. The cell monolayers were washed twice with the incubation medium before the transport experiments. After each wash, the plates were incubated for 30 min at 37°C, and the transepithelial electrical resistance value was determined.

For measurement of the apical to basolateral (A-B) transport, 0.5 mL of the incubation medium containing [^{3}H] uracil of given concentrations was added on the apical side and 1.5 mL of the incubation medium without uracil was added on the basolateral side of the insert. The insert was removed to a well containing fresh incubation medium every 15 min for 1 h. A 150-μL aliquot of the incubation medium was taken from the basolateral side of each well, and the radioactivity was determined by liquid scintillation counting (LSC).

For measurement of the basolateral to apical (B-A) transport, 1.5 mL of the incubation medium containing [^{3}H] uracil of given concentrations was added on the basolateral side and 0.5 mL of the incubation medium without uracil was added on the apical side. The incubation medium in the apical side was replaced with 0.3 mL of fresh medium every 15 min for 1 h. A 300-μL aliquot of the apical side was taken after each replacement, and the radioactivity was measured by LSC.

Uracil was assumed to be stable during the transport experiment (i.e., for 60 min) because no metabolism of the compound has been reported *in vitro* (12), *in situ* (12), or *in vivo* (13).

Uptake Experiments

For measurement of uracil uptake from the apical or basolateral side of the cell monolayer, the incubation medium containing [^{3}H] uracil was added to the apical (0.5 mL) or basolateral (1.5 mL) side, the medium without uracil was added to the opposite sides, and the insert was incubated at 37°C for 2 min. Incubation medium from both sides was removed by aspiration at 0.5, 1, and 2 min. The inserts were washed rapidly twice with 0.5 mL (for the apical side) and 1.5 mL (for the basolateral side) of ice-cold incubation buffer. The monolayers were detached from the insert and transferred to a scintillation vial containing 0.5 mL of cell digestive solution (0.1% w/v Triton X-100 in 0.3 N NaOH). After an overnight digestion, the radioactivity was measured by LSC.

Calculations

The mean transport rate was calculated from the linear portion of the plot of the total amount of uracil transported across the cell monolayer vs. time. A nonlinear regression analysis was performed in the fitting of the plot to a following equation: $V = V_{max} \times S / (K_m + S) + K \times S$, where V is the apparent linear initial rate (pmol/cm^2/min) and S is the initial concentration (μM) in the donor compartment of the insert. V_{max} and K_m are the maximum uptake rate and the Michalis-Menten constant, respectively, and K represents the linear clearance. All data are expressed as the mean ± SD. The statistical significance of differences between treatments was evaluated using the unpaired Student's *t* test.

RESULTS

Effect of Na^+ on the Transport of Uracil across the Caco-2 and LLC-PK_1 Cell Monolayers

The apical to basolateral (A-B) transports of uracil (1 μM) across the Caco-2 and LLC-PK_1 cell monolayers were measured as a function of time in the presence and absence of Na^+ in the apical side (Fig. 1). The transport rates in the absence of Na^+ were 0.15 ± 0.01 and 0.39 ± 0.05 pmol/cm^2/min (n = 3) for the Caco-2 and LLC-PK_1 cell monolayers, respec-

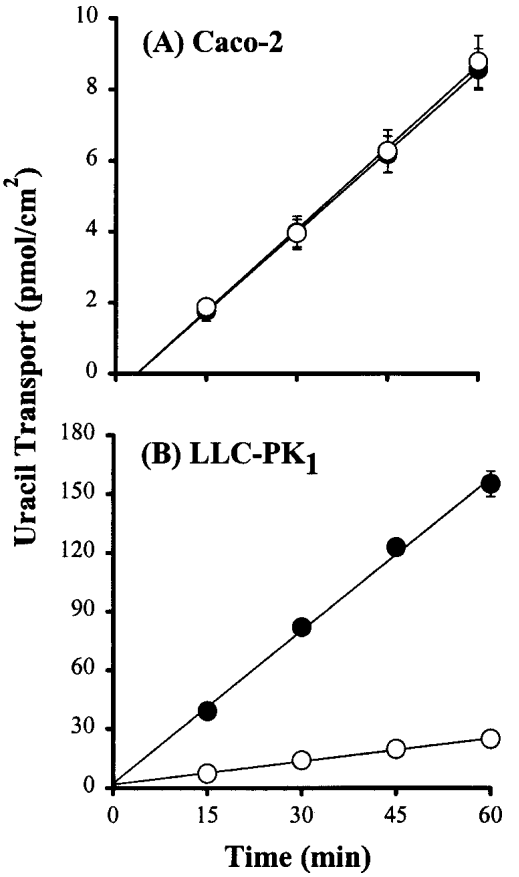

Fig. 1. Effect of Na^+ on the apical to basolateral transport of uracil across the Caco-2 (A) and LLC-PK_1 (B) cell monolayers. The transport was initiated by the addition of 0.5 mL of Na^+-containing (●) or Na^+-free (○) incubation medium (pH 7.4) with [^{3}H] uracil (1 μM) to the apical side of each cell monolayer. Na^+-free incubation medium (pH 7.4, 1.5 mL) without uracil was added to the basolateral side. The appearance of uracil in the basolateral side was measured every 15 min after the incubation at 37°C for a total of 60 min. Each data point represents the mean ± SD of three determinations.

tively. In the presence of Na^+ (140 mM), however, a 7-fold increase in the transport rate of uracil was observed for the LLC-PK$_1$ cell monolayers (i.e., to 2.60 ± 0.11 pmol/cm^2/min, Fig. 1B), whereas no significant change was detected for the Caco-2 cell monolayers (i.e., 0.16 ± 0.02 pmol/cm^2/min, Fig. 1A). These results suggest that the A-B transport of uracil is Na^+ independent in Caco-2 cells and Na^+ dependent in LLC-PK$_1$ cells. In contrast, the basolateral to apical (B-A) transport of uracil were Na^+ independent in both cell lines (data not shown). The transport rates measured in the absence of Na^+ were 0.16 ± 0.01 and 0.46 ± 0.04 pmol/cm^2/min (n = 3) for Caco-2 and LLC-PK$_1$ cell monolayers, respectively.

Concentration Dependency of the Apical to Basolateral Transport of Uracil in Caco-2 and LLC-PK$_1$ Cells

The influence of uracil concentration on the A-B transport of uracil across the Caco-2 cell monolayer was measured in the absence of Na^+ (Fig. 2A). The A-B flux increased with increasing uracil concentration over the concentration range examined (0.4–100 μM). An Eadie-Hofstee plot of the data (inset of Fig. 2A), however, shows that the A-B transport is mediated both by saturable and nonsaturable processes. A nonlinear regression fitting of the data yielded 1.18 μM for K_m, 0.12 pmol/cm^2/min for V_{max}, and 0.19 μL/cm^2/min for K (Table I). The above results indicate that a Na^+-independent, carrier-mediated process, as well as passive diffusion, is involved in the A-B transport.

The influence of uracil concentration on A-B transport of uracil across the LLC-PK$_1$ cell monolayer was examined in the absence or presence of Na^+ in the apical side. In the absence of Na^+, the A-B flux of uracil showed a concentration dependency for the uracil concentration range of 0.4-100 μM (symbol ○ in Fig. 2B). A nonlinear regression of the data yielded a K_m of 50.37 μM, a V_{max} of 16.01 pmol/cm^2/min, and a K of 0.38 μL/cm^2/min (Table I). In the presence of Na^+ (140 mM), a clearer concentration dependency was observed for the A-B flux of uracil for the concentration range of 0.4–100 μM (symbol ● in Fig. 2B). The Na^+-dependent A-B flux of uracil across LLC-PK$_1$ cell monolayers was estimated from the difference in the fluxes between the two experimental conditions (i.e., in the presence and absence of Na^+). A nonlinear regression fitting of the difference (symbol ▲ in Fig. 2B) to a kinetic model involving a saturable process yielded a K_m of 3.67 μM and a V_{max} of 11.31 pmol/cm^2/min (Table I). The above results indicate that both the Na^+-dependent and Na^+-independent carrier-mediated processes, as well as passive diffusion, are involved in the A-B transport of uracil across the LLC-PK$_1$ cell monolayer.

Concentration Dependency of the Basolateral to Apical Transport of Uracil in Caco-2 and LLC-PK$_1$ Cells

It has been suggested that Na^+-independent transport processes are involved in the B-A transport of uracil in both Caco-2 and LLC-PK$_1$ cells. To obtain further information on this issue, we determined the concentration dependency of the B-A transport of uracil in the concentration range of 1–300 μM in a Na^+-free incubation medium (pH 7.4). The B-A flux across Caco-2 cell monolayers exhibited a concentration dependency (not shown) with a K_m of 1.31 μM, a V_{max} of 0.17 pmol/cm^2/min, and a K of 0.21 μL/cm^2/min (Table I).

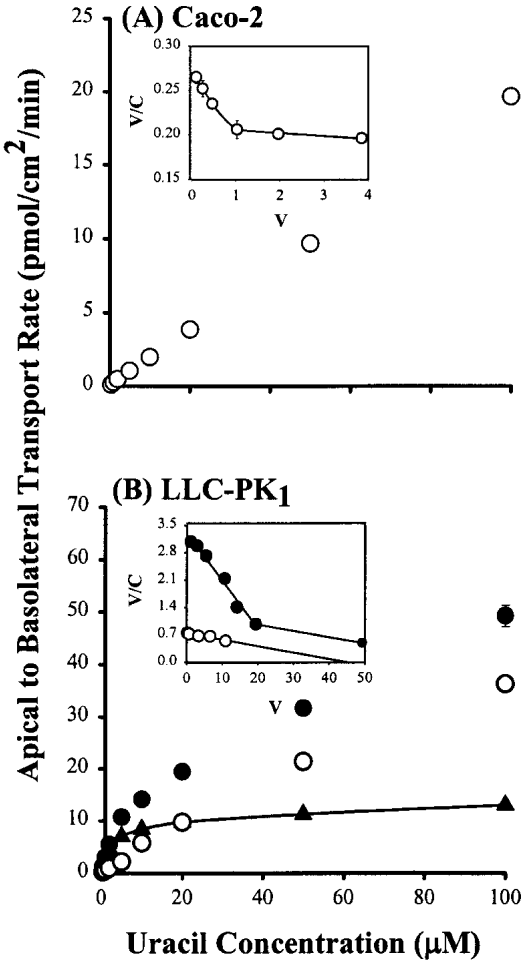

Fig. 2. Concentration dependency of the apical to basolateral transport of uracil across the Caco-2 (A) and LLC-PK$_1$ (B) cell monolayers. The Na^+-containing (●) or Na^+-free (○) incubation medium (pH 7.4, 0.5 mL) with uracil (0.4–100 μM) was added to the apical side, and the transport rate was estimated from the appearance of uracil in the basolateral side (pH 7.4, 1.5 mL) at 15-min intervals for 1 h at 37°C. Na^+-dependent transport (▲) was estimated by subtracting the rate in the Na^+-free medium from that in the Na^+-containing medium. The inset represents the Eadie-Hofstee transformation of the transport data for the cell monolayers. Each data point represents the mean ± SD of three monolayers.

Thus, as in the case of A-B transport, both the Na^+-independent carrier-mediated process and passive diffusion seem to be responsible for the B-A transport of uracil in Caco-2 cells.

Contrary to the case of Caco-2 cells, the B-A transport of uracil was linear for the LLC-PK$_1$ cell monolayer (K: 0.37 μL/cm^2/min, Table I) over the concentration range examined, indicating the absence of carrier-mediated system for the transport.

Mechanism of the Na^+-Dependent, A-B Transport of Uracil in LLC-PK$_1$ Cells

Na^+-dependency was observed only for the A-B transport of uracil across the LLC-PK$_1$ cell monolayer (Fig. 1B and 2B, Table I). To clarify the issue of whether the A-B transport is specifically dependent on Na^+ or not, the effect of three

Table I. Summary of Uracil Transport across Caco-2 and LLC-PK_1 Cell Monolayers[a]

	Caco-2		LLC-PK_1	
	A-B	B-A	A-B	B-A
Na^+ dependent[b]				
K_m (μM)	ND[d]	ND	3.67 ± 0.40	ND
V_{max} (pmol/cm^2/min)	ND	ND	11.31 ± 0.91	ND
Na^+ independent[c]				
K_m (μM)	1.18 ± 0.39	1.31 ± 0.66	50.37 ± 16.91	ND
V_{max} (pmol/cm^2/min)	0.12 ± 0.05	0.17 ± 0.06	16.01 ± 4.48	ND
Passive K (μl/cm^2/min)	0.19 ± 0.01	0.21 ± 0.01	0.38 ± 0.02	0.37 ± 0.03

[a] Data is expressed as the mean ± SD for three monolayers.
[b] Estimated from the difference in the fluxes between the two experimental conditions (i.e., in the presence and absence of Na^+).
[c] Measured in the absence of Na^+.
[d] ND, not determined because of the absence of the process in the transport.

other cations on the transport was examined. For this purpose, NaCl in the incubation medium was replaced by 140 mM KCl, choline chloride, or *N*-methyl-D-glutamine. The A-B transport of uracil (1 μM) was reduced dramatically (up to 7-fold) as a result of the replacement, with no observable differences in the effect among the types of cations in the incubation medium (Table II). This demonstrates that the A-B transport of uracil across the LLC-PK_1 cell monolayer is specifically dependent on Na^+.

To investigate the stoichiometry of the Na^+-dependent transport of uracil, the A-B flux of uracil (1 μM) was measured in the presence of varying concentrations of Na^+ (0–140 mM) in the apical side. In this experiment, the Na^+ concentration in the apical side was varied by reducing the concentration of NaCl, and the iso-osmolarity of the incubation medium was maintained by adding appropriate amounts of *N*-methyl-D-glutamine. The Na^+ free-incubation medium (pH 7.4) was added on the basolateral side. The plot between the Na^+ concentration and the Na^+-dependent A-B flux revealed a hyperbolic stimulation (Fig. 3). The data in Fig. 3 were fitted to Hill's equation shown below (20):

$$\text{Flux} = V_{max}[Na^+]^n/(K_{Na}{}^n + [Na]^n)$$

where K_{Na} is the $[Na^+]$ giving half V_{max} and n is the Na^+:uracil stoichiometry (or Hill coefficient). The nonlinear regression analysis yielded a K_{Na} value of 15.09 ± 2.75 mM and an n of 1.28±0.20 (n = 3, each), respectively, suggesting a Na^+:uracil stochiometry of 1:1. These results indicate that one Na^+ ion is transported per uracil molecule in the A-B transport across LLC-PK_1 cell monolayers.

Table II. Effect of Cations (140 mM Chloride Salts) on the A-B Transport of Uracil (1 μM) across LLC-PK_1 Cell Monolayers[a]

Cation	Uracil transport (pmol/cm^2/min)
Control (Na^+-containing medium)	2.60 ± 0.11
K^+, [b]	0.46 ± 0.05*
Choline$^+$, [b]	0.38 ± 0.03*
NMG$^+$, [b]	0.41 ± 0.05*

[a] Data are expressed as the mean ± SD of three monolayers.
[b] NaCl in the incubation medium (control) was replaced by 140 mM KCl, choline chloride, or N-methyl-D-glutamine (NMG).
* $p < 0.05$ from the control using Student's *t* test.

Effect of Various Compounds on Uracil Transport in Caco-2 and LLC-PK_1 Cells

The substrate specificity for the A-B transport of uracil in both Caco-2 and LLC-PK_1 cells was examined by testing the effect of a variety of compounds (100 μM) on uracil (1 μM) transport. Pyrimidine nucleobases (thymine, 5-fluorouracil), purine nucleobases (hypoxanthine, adenine), nucleobase transport inhibitors (dipyridamole, papaverine, phloridzine), and nucleosides (thymidine, guanosine) were tested for their ability to inhibit uracil transport (Table III). In the case of Caco-2 cells, only adenine and phloridzine inhibited the transport of uracil in the Na^+-free incubation medium ($p < 0.05$). In LLC-PK_1 cells, only thymine and papaverine inhibited the transport in the Na^+-free incubation medium ($p < 0.05$) whereas thymine, 5-fluorouracil, hypoxanthine, papaverine, and phlordzine inhibited the transport in the Na^+ (140 mM)-containing medium ($p < 0.001$).

Polarized Transport of Uracil in Caco-2 and LLC-PK_1 Cells

To better understand the Na^+-independent transport of uracil, the effect of metabolite inhibitors and transport inhibitors on the Na^+-independent uptake of uracil was examined in both Caco-2 and LLC-PK_1 cells (Table IV). In both cells, the uptake of 1 μM uracil in the absence of Na^+ from both the apical and basolateral sides was not influenced by the presence of sodium azide (10 mM) in the donor side, indicating that the Na^+-independent uptake is energy independent. In Caco-2 cells, adenine (100 μM) inhibited the Na^+-independent uracil uptake from the basolateral side whereas in LLC-PK_1 cells, papaverine (100 μM) inhibited the Na^+-

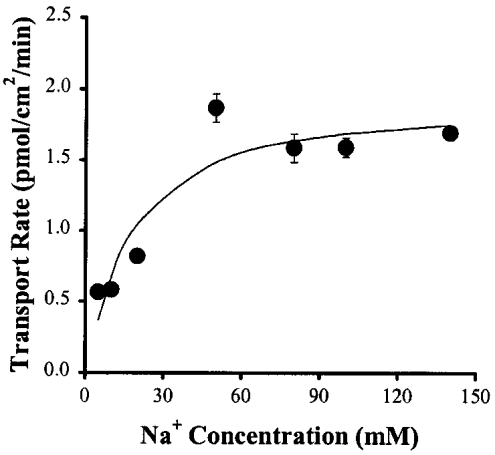

Fig. 3. Effect of Na^+ concentration in the apical side on the apical to basolateral transport of uracil across LLC-PK$_1$ cell monolayers. The incubation medium (pH 7.4, 0.5 mL) containing uracil (1 μM) and varying concentrations (0–140 mM) of NaCl was added to the apical side, and the appearance of uracil in the basolateral side (pH 7.4, Na^+-free medium, 1.5 mL) was measured for 1 h at 37°C. The isoosmolarity of the transport medium in the apical side was maintained by *N*-methyl-D-glutamine. Each data point represents the mean ± SD for three monolayers.

independent uracil uptake from the apical side, possibly indicating that the Na^+-independent transport system is localized on the basolateral membrane of Caco-2 cells and on the apical membrane of LLC-PK$_1$ cells.

The polarity of Na^+-dependent transport in LLC-PK$_1$ cells was further examined (Table IV). In the presence of Na^+ (140 mM), the apical uptake of uracil was 14-fold stimulated compared with the absence of Na^+. However, the basolateral uptake remained unchanged in the absence and presence (data not shown in Table IV) of Na^+, suggesting that the Na^+-dependent uracil transport system is specifically located on the apical membrane of LLC-PK$_1$ cells. In addition, the apical uptake of uracil in the Na^+-containing incubation medium was decreased ($p < 0.05$) by the presence of 10 mM sodium azide, a metabolic inhibitor on the apical side, suggesting that the process is energy dependent. The effect of sodium azide was not observed for the case of basolateral uptake.

DISCUSSION

A previous study demonstrated the presence of two major classes of transporters for the transport of nucleobases, namely equilibrative and concentrative (10). Equilibrative transporters are present in a number of cell types and are broadly selective for purine and pyrimidine nucleobases. Concentrative transporters, e.g., Na^+-dependent nucleobase transporters, have been identified in epithelial cells of several tissues including intestine (11–13), brain (15,16), and kidney (17). The characteristics of the nucleobase transporters seem to vary depending on the tissues and species. In the present study, we examined the characteristics of the transport of uracil, a pyrimidine nucleobase, in Caco-2 and LLC-PK$_1$ cells.

In Caco-2 cells, the A-B transport of uracil was Na^+-independent, consistent with Na^+-independent cellular uptake from the apical side. The transport in both directions (i.e., A-B and B-A) was saturable with comparable K_m and V_{max} values (Table I), suggesting the involvement of the same carrier in both directions. The carrier-mediated transport system in both directions does not appear to be an active system on the basis that no uphill transport of uracil was observed for a specific direction when an insert that contained identical concentrations (1 μM) of uracil on both sides was used (data not shown). In addition, the uracil uptake from the apical and basolateral sides was energy independent (Table IV). The above results suggest that the Na^+-independent transport system of uracil in Caco-2 cells might be a facilitative system. The A-B transport (Table III) and basolateral uptake but not apical uptake (Table IV) was inhibited significantly by the presence of adenine, indicating the probable localization of the facilitative and Na^+-independent uracil transport system on the basolateral membrane of Caco-2 cells.

The Na^+-independent facilitative transport of nucleobases is reported for the first time for Caco-2 cells in the present study. The transport system might be involved in the

Table III. Effect of Nucleosides, Nucleobases, and Their Transport Inhibitors on the A-B Flux of Uracil (1 μM) in Caco-2 and LLC-PK$_1$ Cell Monolayers[a]

	Caco-2 (pmol/cm^2/min)	LLC-PK$_1$ (pmol/cm^2/min)	
Inhibitors[b]	–Na^+ medium	+Na^+ medium[c]	–Na^+ medium
Control	0.22 ± 0.01	2.51 ± 0.17	0.29 ± 0.02
Thymine	0.22 ± 0.03	0.40 ± 0.03***	0.23 ± 0.02*
5-Fluorouracil	0.22 ± 0.01	0.49 ± 0.13***	0.27 ± 0.03
Hypoxanthine	0.21 ± 0.02	0.38 ± 0.01***	0.28 ± 0.04
Adenine	0.19 ± 0.01*	2.77 ± 0.15	0.26 ± 0.03
Dipyridamole	0.24 ± 0.04	2.73 ± 0.11	0.25 ± 0.01
Papaverine	0.25 ± 0.03	1.71 ± 0.18*	0.24 ± 0.01*
Phloridzine	0.19 ± 0.02*	1.67 ± 0.09*	0.25 ± 0.03
Thymidine	0.24 ± 0.02	2.60 ± 0.20	0.25 ± 0.03
Guanosine	0.23 ± 0.01	2.24 ± 0.49	0.27 ± 0.02

[a] Data are expressed as the mean ± SD of three monolayers.
[b] Inhibitor concentration used in these experiments was 100 μM.
[c] The concentration of Na^+ was 140 mM.
* $p < 0.05$ from the control using Student's *t* test.
*** $p < 0.001$ from the control using Student's *t* test.

Table IV. Apical and Basolateral Uptake of Uracil (1 μM) in Caco-2 and LLC-PK_1 Cell Monolayers[a]

Incubation Condition	Caco-2 (pmol/cm^2/min)		LLC-PK_1 (pmol/cm^2/min)		
	Apical	Basolateral	Apical		Basolateral
	$-Na^+$ medium		$+Na^+$ medium[b]	$-Na^+$ medium	$-Na^+$ medium
Control	230.5 ± 48.4	932.4 ± 33.3	1870.98 ± 263.41**	130.23 ± 18.53	143.41 ± 22.71
NaN_3[c]	244.3 ± 25.7	936.9 ± 38.2	883.10 ± 154.43*	123.33 ± 22.33	163.16 ± 22.02
Adenine[d]	236.2 ± 29.7	793.5 ± 17.2*	ND	ND	ND
Papaverine[d]	ND[e]	ND	ND	89.80 ± 11.46*	114.67 ± 19.15

[a] Data are expressed as the mean ± SD of three monolayers.
[b] The concentration of Na^+ was 140 mM.
[c] The concentration used in these experiments was 10 mM.
[d] The concentration used in these experiments was 100 μM.
[e] ND, not determined.
* $p < 0.05$ from the control using Student's *t* test.
** $p < 0.05$ from the $-Na^+$ medium using Student's *t* test.

salvage of purine for nucleic acid synthesis in the intestine. A Na^+-dependent transport system was not observed for the transport of uracil in Caco-2 cells, contrary to previous studies that reported the involvement of a Na^+-dependent system for the transport of uracil (11) and 5-fluorouracil (13,14) across the small intestine of rats. In this regard, Caco-2 cells may not represent an appropriate model for the Na^+-dependent transport of nucleobases in the small intestine *in vivo*.

In LLC-PK_1 cells, the A-B transport of uracil was specifically dependent on Na^+ (Tables I and II). Collectively, a uracil/Na^+ symport system seems to be a prevalent mechanism for the A-B transport of uracil in LLC-PK_1 cell monolayers on the basis of the 10-fold larger clearance of the Na^+-dependent transport compared with Na^+- independent transport (3.1 vs. 0.3 μL/cm^2/min from V_{max}/K_m in Table I). The Na^+-dependent A-B transport of uracil was saturable and exhibited a high affinity (K_m of 3.67 μM, Table I) for the transport system with a Na^+:uracil coupling stoichiometry of 1:1 (Fig. 3), suggesting the presence of a single Na^+ binding site on the relevant transporter protein. In addition, an uphill transport of uracil was observed in the A-B direction, reaching a 1.5-fold higher basolateral concentration compared with the apical concentration in 1 h (data not shown). Moreover, the uracil uptake from the apical side but not from the basolateral side was significantly inhibited when the LLC-PK_1 cells were incubated with sodium azide, a metabolic inhibitor (Table IV). As mentioned in the Results section, the presence of Na^+ increased the A-B transport (Fig. 1B) and the apical uptake (Table IV) up to 7- and 14-fold, respectively, but not the basolateral uptake. Thus, the active and Na^+-dependent uracil transport system seems to be localized on the apical membrane of LLC-PK_1 cells. A Na^+-dependent transport system has been reported in LLC-PK_1 cells for the apical uptake of hypoxanthine, a purine nucleobase (17). The system was inhibited by thymine, 5-fluorouracil, and hypoxanthine but not by adenine (17), as in the case of the Na^+-dependent A-B transport of uracil (Table III), suggesting the involvement of a common system in the transport of uracil and hypoxanthine. Hypoxanthine, in that case, seems to exhibit 4.7-fold higher affinity (i.e., K_m of 0.79 μM) to the system compared with uracil (i.e., K_m of 3.67 μM, Table I).

In addition to Na^+-dependent uracil transport system, a Na^+-independent carrier-mediated process with an apparent K_m (50.37 μM) and V_{max} (16.01 pmol/cm^2/min) seems to be involved in the A-B transport of uracil in LLC-PK_1 cells (Table I). The A-B transport of uracil, a pyrimidine nucleobase, was inhibited by the presence of thymine, a pyrimidine nucleobase, but not by the presence of hypoxanthine and adenine, purine nucleobases (Table III), consistent with the preferential transport of hypoxanthine by the purine nucleobase transport system in LLC-PK1 cells (17). In human erythrocytes (21), however, a Na^+-independent purine nucleobase transport system is involved in the transport of pyrimidine nucleobases (e.g., 5-fluorouracil and uracil). Thus, the substrate specificity of nucleobase transporters seems to vary depending on the cell line. On the other hand, the Na^+-independent uracil uptake from apical and basolateral sides was energy independent (Table IV) and no uphill transport of uracil was observed across the LLC-PK_1 cell monolayers (data not shown), suggesting the involvement of a facillitated mechanism in the transport of uracil in LLC-PK_1 cells. The apical uptake of uracil but not the basolateral uptake was inhibited by the presence of papaverine, a nucleobase transport inhibitor (Table IV), indicating the localization of the Na^+-independent transport system on the apical membrane. This is quite different from the general cases, in which the two processes (i.e., Na^+-independent and Na^+-dependent transport systems) are asymmetrically distributed on the apical and basolateral membranes, coordinating the vectorial transepithelial transport of substrates, as represented by the absorption of glucose across the intestinal epithelial cell. The difference might be associated with the lower affinity of uracil to the Na^+-independent transport system on the basolateral membrane compared with the apical membrane (17,18).

In summary, the transport of uracil in Caco-2 cells seems to be mediated by a Na^+-independent facilitated transport system, and the system seems to be localized on the basolateral membrane. In LLC-PK_1 cells, the A-B transport of uracil involved both Na^+-dependent and Na^+-independent processes. Both the high-affinity, active Na^+-dependent process and facilitative, Na^+-independent process were localized on the apical membrane. The above mechanisms may be involved in the salvage of pyrimidine nucleobases including uracil from the extracellular fluid in the small intestine, and the reabsorption of these compounds from the renal proximal tubules.

ACKNOWLEDGMENT

This research was supported in part by a grant (HMP-99-D-07-0004) from the Ministry of Health and Welfare, Republic of Korea.

REFERENCES

1. P. G. W. Plagemann, R. M. Wohlhueter, and C. Woffendin. Nucleoside and nucleobase transport in animal cells. *Biochim. Biophys. Acta* **94**:405–443 (1988).
2. F. M. Sirotnak and J. R. Barrueco. Membrane transport and the antineoplastic action of nucleoside analogue. *Cancer Metastasis Rev.* **6**:459–480 (1987).
3. M. S. Hwang, S. J. Lee, K. S. Song, C. S. Kim, B. Y. Lee, and J. W. Lee. Kinetic studies of a novel reversible H^+ pump antagonist, YH1885, on H^+/K^+-ATPase. *The Spring Convention of the Pharmaceutical Society of Korea.* 1998, April 24-25, Pusan, Korea.
4. P. G. W. Plagemann and M. Kraupp. Inhibition of nucleoside and nucleobase transport and nitrobenzylthioinosine binding by dilazep and hexobendine. *Biochem. Pharmacol.* **35**:2559–2567 (1986).
5. M. Kraupp and R. Marz. Membrane transport of nucleobases: Interaction with inhibitors. *Gen. Pharmc.* **26**:1185–1190 (1995).
6. U. Lonn, S. Lonn, U. Nylen, and G. Winblad. 5-fluoropyrimidine induced DNA damage in human colon carcinoma and its augmentation by the nucleoside transport inhibitor dipyridamole. *Cancer Res.* **49**:1085–1089 (1989).
7. K. Isono. Current progress on nucleoside antibiotics. *Pharmacol. Ther.* **52**:269–286 (1991).
8. W. Sun and D. Haller. UFT in the treatment of colorectal and breast cancer. *Oncology (Huntingt)* **15:**49–56 (2001).
9. M. A. Afifi, H. S. el-Wakil, and M. M. Abdel-Ghaffar. A novel chemotherapeutic combination for trichomonas vaginalis targeting purine slavage pathways of parasite. *J. Egypt. Soc. Parasitol.* **30**:735–746 (2000).
10. D. A. Griffith and S. M. Jarvis. Nucleoside and nucleobase transport systems of mammalian cells. *Biochim. Biophys. Acta* **1286**: 153–181 (1996).
11. J. R. Bronk, N. Lister, and S. Lynch. Absorption of 5-fluorouracil and related pyrimidines in rat small intestine. *Clin. Sci.* **72**:705–716 (1987).
12. H. Sasaki, J. Nakamura, R. Konishi, and J. Shibasaki. Intestinal absorption characteristics of 5-fluorouracil, ftorafur and 6-mercaptopurine in rats. *Chem. Pharm. Bull.* **34**:4265–4272 (1986).
13. J. R. Bronk and J. G. Hastewell. The transport pyrimidines into tissue rings cut from rat small intesine. *J. Physiol.* **382**:475–488 (1987).
14. H. Yuasa, E. Matsuhisa, and J. Watanabe. Intestinal brush border transport mechanism of 5-fluorouracil in rats. *Biol. Pharm. Bull.* **19**:94–99 (1996).
15. C. B. Washington and K. M. Giacomini. Mechanisms of nucleobase transport in rabbit choroid plexus. *J. Biol. Chem.* **270**:22816–22819 (1995).
16. C. B. Washington and K. M. Giacomini. Mechanisms of 5-fluorouracil (5-FU) transport in isolated rabbit choroid plexus tissue slices. *Pharm. Res.* **13**:1276–1278 (1996).
17. D. A. Griffith and S. M. Jarvis. High affinity sodium-dependent nucleobase transport in cultured renal epithelial cells (LLC-PK1). *J. Biol. Chem.* **268**:20085–20090 (1993).
18. D. A. Griffith and S. M. Jarvis. Characterization of a sodium-dependent concentrative nucleobase-transport system in guinea-pig kidney cortex brush-border membrane vesicles. *Biochem. J.* **303**:901–905 (1994).
19. H. Li, S. J. Chung, D. C. Kim, H. S. Kim, J. W. Lee, and C. K. Shim. The transport of reversible proton pump antagonist, 5, 6-dimethyl-2-(4-fluorophenylamino)-4-(1-methyl-1,2,3,4-tetrahydroisoquinoline-2-yl) pyrimidine hydrochloride (YH1885), across Caco-2 cell monolayers. *Drug Metab. Dispos.* **29**:54–59 (2001).
20. I. H. Segel. Enzyme Kinetics. Wiley, New York, 1975 pp. 360–374.
21. B. A. Domin, W. B. Mahony, and T. P. Zimmerman. Purine nucleobase transport in human erythrocytes. *J. Biol. Chem.* **263**: 9276–9284 (1988).